



## NANONIZED CURCUMIN IMPROVED ORAL BIOAVAILABILITY OF BROMOCRIPTINE THROUGH CYP3A ENZYME INHIBITION IN RATS

Kankalatha Alikatte<sup>1,2</sup>, Rajeshre Dhurke<sup>2</sup>, Sashidhar R.B\*<sup>1</sup>

<sup>1</sup>Department of Biochemistry, University College of Science, Osmania University, Hyderabad, Telangana, India

<sup>2</sup>Department of Pharmacology, St. Peters Institute of Pharmaceutical Sciences, Warangal, Telangana, India

<sup>3</sup>Department of Pharmaceutics, St. Peters Institute of Pharmaceutical Sciences, Warangal, Telangana, India

\*Corresponding author: [sashi\\_rao@yahoo.com](mailto:sashi_rao@yahoo.com)

### ABSTRACT

Curcumin (CUR) a water insoluble dietary flavonoid and is reported to inhibit CYP3A4 enzyme. The objective of present study was to assess the effect of CUR and nanonized curcumin (NC) on bromocriptine (BRO) metabolism in rats. NC was prepared by antisolvent precipitation method and was evaluated for particle size and solubility. CYP3A inhibitory activity of CUR was assessed *in vitro* using erythromycin-N-demethylase (EMD) assay. CYP3A inhibitory effect of CUR and NC confirmed *in vivo* using pharmacokinetic study of midazolam. These findings were further confirmed by an *in vivo* pharmacokinetic study in which BRO was administered (10 mg/kg, p.o) to CUR and NC (60 mg/kg, p.o.) pretreated (10 days) rats and its plasma concentrations were determined by HPLC analysis. CUR significantly ( $p < 0.05$ ) inhibited CYP 3A activity in EMD assay. CUR and NC significantly ( $p < 0.05$ ) increased plasma concentrations of midazolam in dexamethasone pretreated rats. In addition, *in vivo* studies revealed that CUR and NC pretreatments significantly ( $p < 0.05$ ) increased  $C_{max}$  and AUC and decreased CL/F of BRO compared with BRO group. NC pretreatment may increase the bioavailability of BRO which could be mediated through the inhibition of CYP 3A enzymes.

**Keywords:** Curcumin, Bioavailability, Bromocriptine, Cytochrome P4503A enzyme, Microsomal enzymes.

### 1. INTRODUCTION

Bromocriptine (BRO) is an ergoline derivative and a potent D<sub>2</sub>-dopamine agonist, directly or indirectly protecting dopaminergic cells. BRO is used in the treatment of Parkinson's disease, pituitary tumors, galactorrhea, infertility, acromegaly, amenorrhea, neuroleptic malignant syndrome, type 2 diabetes and prolactinomas [1]. BRO is available in oral dosage forms and is easily absorbed through the gastrointestinal tract. Due to extensive first-pass effect, only 6% of oral dose reaches the systemic circulation [2]. BRO is extensively metabolized by the Cytochrome P4503A (CYP3A) enzymes [3]. It was earlier reported that BRO concentration in systemic circulation was observed to increase with CYP3A inhibitors like macrolide antibiotics, protease inhibitors or anti-fungal therapies [4]. Curcumin (CUR) is a hydrophobic polyphenol derived from the rhizome of the herb *Curcuma longa*. It has a wide spectrum of biological and pharmacological activities [5]. Traditionally, it has been widely used in Ayurveda, Unani, and Siddha medicine to cure various

diseases. It possesses potent antioxidant [6], anti-inflammatory [7], and anti-cancer activities [8], thus, exhibits beneficial health effects on various diseases, including multiple myeloma, pancreatic cancer, myelodysplastic syndromes, colon cancer, psoriasis, arthritis, major depressive disorder, and Alzheimer's disease [9]. In spite of its promising therapeutic index, the biological activity of CUR is severely limited due to its poor bioavailability and hence has not yet been approved as a therapeutic agent. Effective methods to deliver such substances to increase their bioavailability have been a major challenge in current biomedical and food research [5].

Oral administration is the most common and usually preferred drug delivery method, especially in patients who need long term treatment for their chronic illness [10]. CYP3A enzymes are important subfamily of CYP isoforms contribute to the first-pass metabolism as a result reduced the oral bioavailability of many drugs [11]. CUR has been reported to inhibit *in vitro* CYP1A2, 2B6, 2C9, 2D6, and 3A4 activities in human cDNA-

expressed CYP enzymes [12]. In rats, CUR (60 mg/kg/day) treatment for 4 days significantly reduced the protein expression of intestinal CYP3A and P-gp [13]. Therefore, use of CYP3A inhibitors along with orally administered CYP3A substrate drugs greatly improves the bioavailability.

Over the past two decades, nanotechnology as a novel approach in the area of pharmaceuticals, finds newer applications. One of its major benefits is improving bioavailability of poorly soluble drugs [14]. Nanoparticles are particularly suitable for drug delivery of water insoluble compounds. In this study, Nanonization of CUR was done by antisolvent precipitation method using syringe pump (APSP) in order to improve the solubility there by increasing the oral bioavailability of CUR. As a result, the residence time of CUR in systemic circulation greatly improved and a potential possibility for pharmacokinetic interaction with concomitantly administered drug.

The key objective of this study was to improve the oral bioavailability of BRO with the use of nanonized curcumin (NC), which inhibits CYP3A enzymes, subsequently affecting the metabolism of BRO.

## 2. MATERIAL AND METHODS

### 2.1. Chemicals

Bromocriptine and curcumin was purchased from Sigma-Aldrich (Bangalore, India), Dexamethasone and midazolam were gifted by Wochardt Research Center, Aurangabad, India. Potassium dihydrogen phosphate, absolute ethanol (99.5-99.8%), acetone and acetonitrile (HPLC grade) were obtained from Merck Specialties Pvt. Ltd, (Mumbai, India). Solvents used for quantitative analysis and all other chemicals, reagents which were used in the study, are of analytical grade.

### 2.2. Animals

The study was performed on male wistar rats (150-250 g). The rats were kept in polyacrylic cages and maintained under standard laboratory conditions (room temperature 24-27°C and humidity 60-65%). They were fed with standard pellet diet and water *ad libitum*. Handling and experimentation were conducted in accordance with the approved guidelines of the Committee for the Purpose of Control and Supervision of Experiments on Animals (CPCSEA), New Delhi. All in vivo animal experimental protocol conducted in this study were approved (06/SPIPS/IAEC/19) by the Institutional Animal Ethical Committee, Kakatiya University, Warangal.

### 2.3. Preparation of Nanonized curcumin (NC)

NC was prepared by antisolvent precipitation with a syringe pump (APSP) method. In this method, CUR was dissolved in acetone at concentration of 10 mg/mL. The prepared solution (20 mL) was filled into a syringe and was secured onto a syringe pump. The drug solution was quickly injected at a fixed flow rate (2-10 mL/min) into the deionized water (antisolvent) of a definite volume (solvent/antisolvent ratio-1:15) under magnetic stirring (1,000 rpm). NC formed from this method was filtered and vacuum dried [15].

### 2.4. Characterization of NC

#### 2.4.1. Particle Size and Zeta Potential

To measure the mean nanoparticle size and size distribution; dynamic light scattering (DLS) was employed (Nanotracer wave w3231, Japan). DLS measurements were performed at 532 nm wavelength, at 25°C with an angle of detection of 173° after suitable dilution with distilled water. Zeta potential was recorded from the same instrument [16]. The surface charge is dependent on the zeta potential ( $\zeta$ ), which is developed when a solid powder is dispersed in a liquid. The zeta potential explains the degree of repulsion between like charge neighbouring particles in dispersion [17]. The physical stability of nanoparticle formulation was determined by zeta potential. Lower values nearer to zero indicate agglomeration/aggregation resulting in physical instability [18].

#### 2.4.2. Scanning electron microscopy (SEM)

Surface and shape characteristics of CUR and NC were evaluated by scanning electron microscopy (SEM) Zeiss EVO 18-EDX special edition instrument compatible with EDX machine. The powder samples were spread on a SEM stub and sputtered with gold before the SEM observations. The particle size and texture of nanoparticles was analyzed by using image magnification software compatible with SEM that aids in determining the presence and formation of NC. Five SEM pictures were used to find the average range of particle diameter.

#### 2.4.3. Differential Scanning Calorimetry (DSC)

Differential scanning calorimetry was performed using DSC- 60, Shimadzu instrument. DSC thermograms were obtained using an automatic thermal analyzer system. Samples were crimped in standard aluminum pans and heated from 0 to 400°C at a heating rate of 10°C/minutes under constant purging of dry nitrogen

at 30 mL/minutes. For analysis, 5 mg of drug i.e. CUR and NC was used for the study. The resultant thermograms were recorded.

#### 2.4.4. *In vitro* dissolution studies

The *in vitro* dissolution of the CUR (5 mg) and NC (5mg) were determined using the paddle method (Vankel VK 7000 Dissolution Tester, USA) in 100 mL of simulated intestinal fluid (SIF) at pH 6.8 [19]. The paddle rotation was set at 100 rpm and temperature was maintained at  $37\pm 0.5^{\circ}\text{C}$ . The dissolved solution samples of 1 mL were collected at 15, 30, 45, 60, 90, 120 and 180 min of dissolution time. For each sample the dissolution test was performed thrice. The concentration of drug was determined spectrometrically at 422 nm using UV spectrometer (UV-3101PC, Shimadzu, Japan) [15].

### 2.5. Study design

#### 2.5.1. *In vitro* assessment of CYP3A activity in liver and intestine [20]

This method is based on the principle that CYP3A converts erythromycin to N-demethyl erythromycin and formaldehyde, which produces yellow colour with Nash reagent [21]. After overnight fasting, rats were euthanized by pentobarbitone overdose. Liver was perfused with 10 mL of 0.1 M phosphate buffered saline (PBS) and then isolated. Similarly, a piece of small intestine (10 cm long) was isolated and washed with PBS.

We used this assay to check the inhibitory effect of CUR on CYP3A enzymes. In this method, we have not included NC as it is an *in vitro* enzyme inhibition assay where improvement of CUR bioavailability is not pertinent.

#### 2.5.2. Preparation of intestinal microsomes

A method validated by Cotreau et al. and Takemoto et al. [22, 23] was employed with minor modifications to prepare intestinal microsomes. Each isolated intestinal segment (0.5g) was cut into pieces, washed with ice cold PBS and then cut longitudinally to expose mucosa. The mucosal layer was scraped lightly from all pieces of intestine with the help of a glass cover slip. All scrapings were mixed together and centrifuged 5 min. The pellet was suspended in 5.0 mL of ice cold histidine-sucrose buffer (HSB) (histidine 5 mM, pH 7.0; sucrose 0.25 M; NaEDTA 0.5 mM; pH 7.4); homogenized and centrifuged at  $15,000 \times g$  for 10 min. The supernatant was carefully transferred to a clean tube. The pellet was

resuspended in 5.0 mL of HSB and again centrifuged at  $15,000 \times g$  for 10 min. The supernatant after each centrifugation was taken together and mixed with 52 mM  $\text{CaCl}_2$  (0.2 mL per mL of the supernatant) to precipitate microsomes. After 15 min of standing, it was centrifuged at  $20,000 \times g$  for 15 min, the microsomal pellet was suspended in 0.5 mL of 0.1 M potassium phosphate buffer (pH 7.0) containing 20% glycerol, and stored at  $-20^{\circ}\text{C}$  until use. Protein concentration of the microsomal fraction was determined by Biuret method [24] using bovine serum albumin as the standard.

#### 2.5.3. Preparation of liver microsomes

The liver microsomes were prepared by minor modification of the method proposed by Schenkman and Cinti [25]. The liver isolated from rats was minced and homogenized in appropriate amount of 0.25 M sucrose containing 10mM Tris-HCl (pH 7.5), and then centrifuged at  $600 \times g$  for 5 min. The post-mitochondrial supernatant was separated, mixed with solid  $\text{CaCl}_2$  so that its concentration in the given volume of supernatant was 8.0 mM and then centrifuged at  $12,000 \times g$  for 10 min. The pellet so obtained was resuspended in mixture of 150 mM KCl-10mM Tris-HCl (pH 7.5), and centrifuged at  $20,000 \times g$  for 20 min to obtain pinkish microsomal pellet, which was suspended in 0.5 mL of 0.1 M potassium phosphate buffer containing 20% glycerol and stored at  $-20^{\circ}\text{C}$  until use. Protein concentration of samples was determined by Biuret [24] method using bovine serum albumin as the standard.

#### 2.5.4. Erythromycin-N-demethylation assay

The mixture of microsomal protein (0.5mg), erythromycin (0.1mL, 10 mM) and potassium phosphate (0.6 mL, 100 mM, pH 7.4) was incubated at  $37^{\circ}\text{C}$  along with CUR at a concentration of 0.1, 1 and 10  $\mu\text{M}$ . The reaction between these agents was initiated by adding NADPH (0.1mL, 10 mM), and terminated after 10 min, by adding ice cold trichloroacetic acid (0.5 mL, 12.5% w/v) solution. It was centrifuged ( $2000 \times g$ ; 10 min) to remove proteins. To 1 mL of this supernatant, 1mL of Nash Reagent (2 M ammonium acetate, 0.05 M glacial acetic acid, 0.02 M acetyl acetone) was added, and heated in a hot water bath at  $50^{\circ}\text{C}$  for 30 min. After cooling, the absorbance was read at 412 nm in a spectrophotometer. The activity was calculated from standards (0-1  $\mu\text{M}$  formaldehyde) prepared by substituting sample with standard solution

which were run in parallel. CYP3A activity was calculated using the following formula:

CYP3A activity = Amount of formaldehyde produced (nmol $\times$ 1/0.5mg $\times$ 1/30 min.). The CYP3A activity was expressed as nM of formaldehyde formed per milligram of protein per min.

#### 2.5.5. *In vivo* CYP 3A activity assay

*In vivo* CYP3A activity was assessed by using a model developed by Kanazu et al [26]. The method is based on the principle that midazolam being a substrate for CYP3A, the activity of this enzyme inversely reflects upon the plasma levels of orally administered midazolam. Artificially CYP3A activity was induced by dexamethasone pretreatment so that the inhibitory effect of any agent would better reflect on midazolam levels.

Rats were divided into five groups (n=6), first group received vehicle (0.5% methylcellulose in water) and served as dexamethasone untreated control while remaining four groups received dexamethasone (80 mg/kg ip) daily in three divided doses for three consecutive days. Second group served as dexamethasone group. Third and fourth group of animals were pre-treated with CUR and NC (60 mg/kg, p.o) for 10 days. Fifth group received ketoconazole, 5 mg/kg (standard) on day 11. On day 11, after 1 h of CUR, NC and ketoconazole administration, midazolam (20 mg/kg, p.o.) was administered. Blood samples (0.3 mL) were collected in heparinized Eppendorf tubes at 30 min, 1, 1.5, 2 and 4 h through tail vein and centrifuged immediately at 3000 $\times$ g for 15 min to separate plasma which was stored at -20 $^{\circ}$ C until analysis.

The plasma concentration of orally administered midazolam was determined by HPLC [27]. In brief, plasma (0.1mL), internal standard (0.1mL of diazepam; 80 ng in methanol) and NaOH (0.5 mL, 1N) were mixed together. Then n-hexane (3.0mL) was added to the mixture, vortex mixed for 5 min and later centrifuged at 10,000  $\times$ g for 5 min. The upper layer (3.0mL) was separated and evaporated under vacuum. The residue was dissolved in 100  $\mu$ L of mobile phase and 20  $\mu$ L was injected onto the HPLC system for analysis. The UV-detector was set at 230 nm. SYMMETRY1 C8 column (4.6mm $\times$ 150mm, 5 mm particle size, Waters Co., Milford, USA) was used at a temperature of 30 $^{\circ}$ C. Mobile phase consisted of 0.1mM sodiumacetate buffer (pH4.7) and acetonitrile in a ratio of 60:40 (v/v). The flow rate was maintained at 1.0

mL/min. The method was linear in the range of 50-10,000 ng/mL. The average recovery of the drug was 92.3%. The intra-day and inter-day coefficients of variation for the low and high quality control samples were <9%.

#### 2.5.6. *In vivo* pharmacokinetic study

Rats were fasted for at least 12 h prior to experiments and approximately 3 h post-dose. The rats were divided into 3 groups consisting of six animals each. Group I was administered with BRO (10 mg/kg; p.o.) on the 11th day. Group II was pretreated with CUR (60 mg/kg; p.o.) for 10 days and on the 11th day with BRO (10 mg/kg) followed by CUR (60 mg/kg; p.o.), and group III was pretreated with NC (60 mg/kg; p.o.) for 10 days and on the 11th day with BRO (10 mg/kg) followed by NC (60 mg/kg; p.o.). Under ether anesthesia, blood samples (approximately 0.25 mL) were collected from the retro-orbital plexus into heparinized micro centrifuge tubes prior to dose and at 0.5, 1, 1.5, 2, 3, 4, 6, 8, 10 and 12 h post-dose. The blood samples were centrifuged at 15000  $\times$  g for 15 min. The plasma samples were stored at -20 $^{\circ}$ C until the HPLC analysis.

#### 2.5.7. HPLC analysis of BRO

The drug analysis of samples was carried out using Shimadzu HPLC system equipped with a LC-20AD pump, SPD 20A UV visible detector, Rheodyne injector port (20  $\mu$ L loop) and RP C18 column (Phenomenex Luna, 250 mm  $\times$  4.6 mm ID, particle size 5 mm). The mobile phase comprised of acetonitrile- water (0.2% triethylamine) (70: 30 v/v), adjusted to pH 3 with HCL. Analyses were run at a flow rate of 1 mL/min and the elution was monitored at 280 nm [28].

*In vitro* and *in vivo* plasma samples were extracted using a simple protein precipitation method by adding acetonitrile (200  $\mu$ L) to samples (100  $\mu$ L). Additionally 100  $\mu$ L of verapamil (100 ng/mL) was added to *in vivo* samples as an internal standard. Samples were mixed in a vortex mixer for 2 min and centrifuged at 15,000 $\times$ g for 15 min. The resultant clean supernatant (20  $\mu$ L) was injected and analyzed using HPLC method. The peak area ratios obtained at different concentrations of the drug and internal standard were plotted against the concentration of drug. The limit of detection (LOD) was 0.01 $\mu$ g/mL and the assay range used was 0.01-10  $\mu$ g/mL. The average recovery of the drug was 91.7%. The intra-day and inter-day coefficients of variation for

the low and high quality control samples were less than 10%.

### 2.5.8. Pharmacokinetic analysis

Pharmacokinetic parameters were computed by the non-compartmental model using Phoenix Win Nonlin version 6.2 software (Certara, Pharsight Corporation, USA). The maximum plasma concentration (C<sub>max</sub>) and the time to reach the maximum plasma concentration (T<sub>max</sub>) were determined by a visual inspection of the experimental data. The plasma BRO concentration *versus* time plots were used to estimate the area under the concentration-time curve to the last sampling point (AUC<sub>0-t</sub>), area under the concentration-time curve to the infinity (AUC<sub>0-∞</sub>), half-life (T<sub>1/2</sub>), elimination rate constant (K<sub>el</sub>), clearance (CL/F) and volume of distribution (V<sub>d</sub>/F).

### 2.6. Statistical analysis

All mean values are presented along with their standard

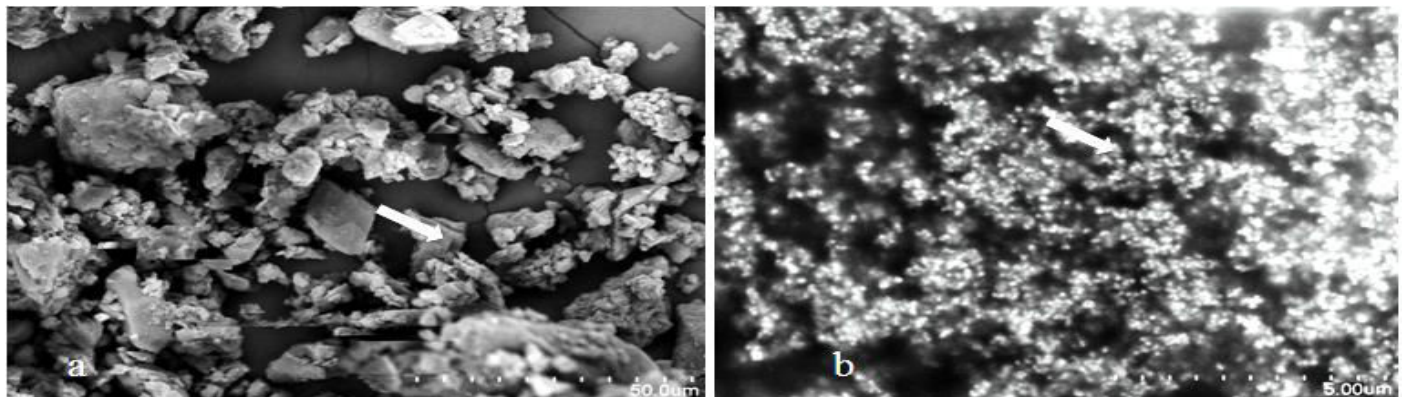
deviation (mean SD). Statistical analysis was performed using Student's unpaired t-test and analysis of variance (ANOVA) using Graph Pad Prism version 5.0 (GraphPad Software Inc., San Diego, CA, USA) at significance level of  $p < 0.05$ .

## 3. RESULTS

### 3.1. Characterisation of NC

#### 3.1.1. SEM and zeta potential analysis

SEM imaging of the CUR and NC (fig.1a, fig.1b) shows the morphological characteristics of the CUR. As observed, CUR exhibited much larger particles of irregular shapes and lacking size uniformity. In contrast, NC was regular, spherical in shape and more uniform in size and shape. Curcumin particles were found to be in the range of 1-2.5 μm. After nanonization, the majority of particles were found to be in the range of 40-50 nm (fig.1C.). The zeta potential of NC was observed to be in the range of -15 to -20MV, suggesting an enhanced physical stability of NC.



a) SEM image indicating the morphology of curcumin before nanonization (magnification, 50 μm) b) SEM image indicating the morphological changes in curcumin after nanonization (nanonized curcumin) (magnification, 5 μm)

**Fig. 1: Scanning electron microscopic images of curcumin and nanonized curcumin prepared by APSP**

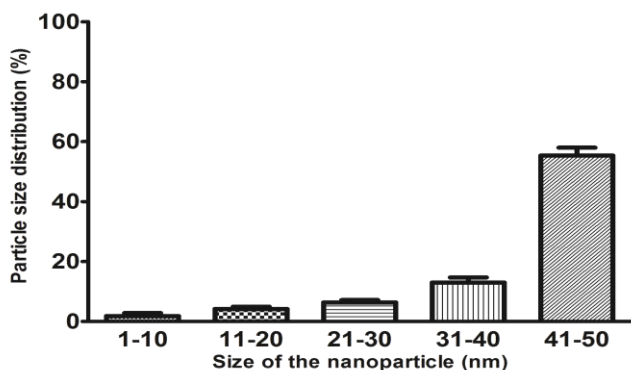


**Fig. 1C: Particle size distribution of nanonized curcumin**

#### 3.1.2. DSC

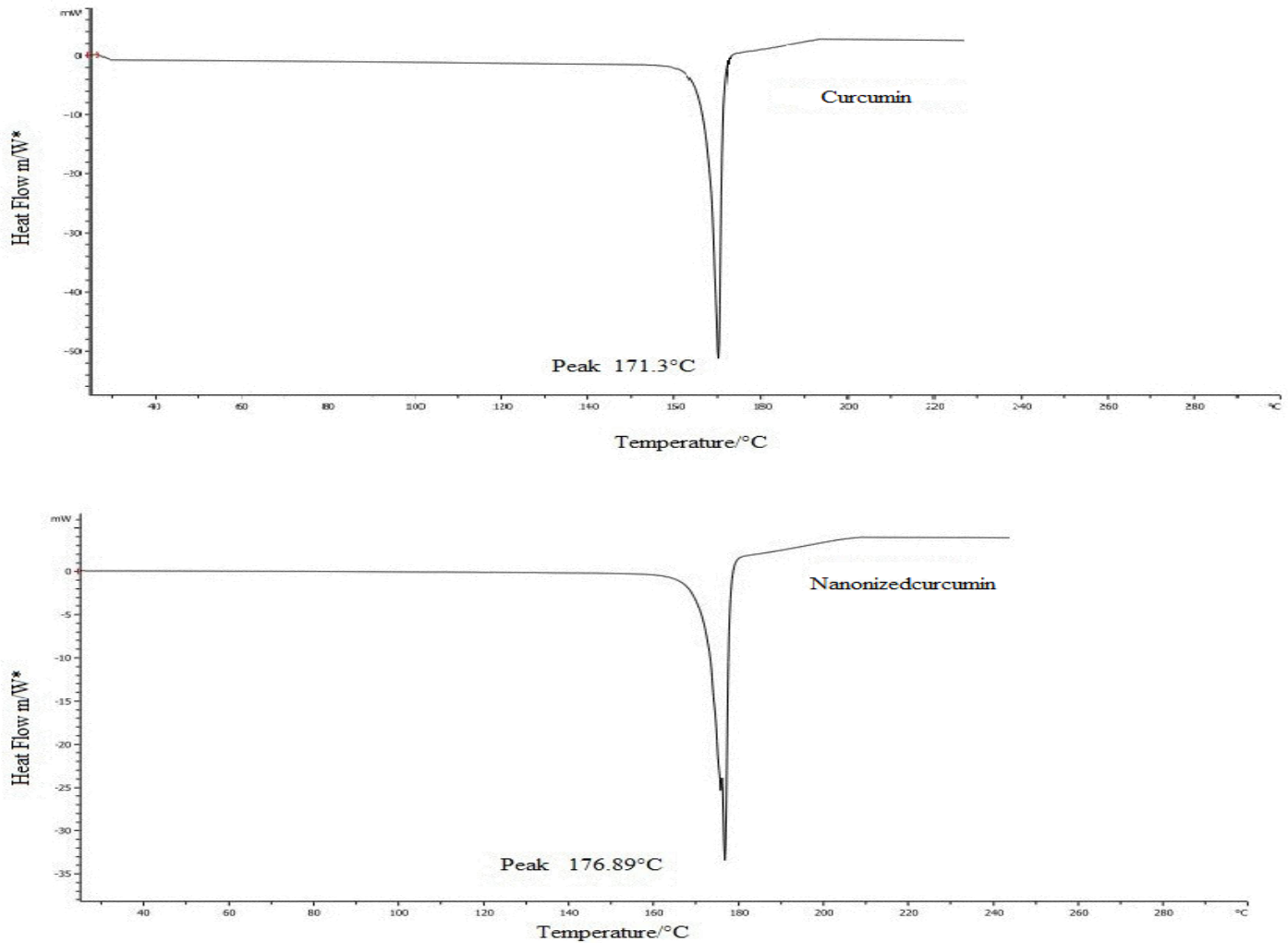
Thermograms of CUR and NC were recorded and are shown in fig. 2. CUR showed a sharp melting endothermic peak at 171.3°C, and a melting enthalpy of fusion 160.7 J/g, whereas NC showed melting endothermic peak at 176.89°C but the melting enthalpy of fusion was lower (65.1 J/g) than that of the CUR. The enthalpy of fusion is proportional to the degree of crystallinity in the samples, suggested that the crystallinity of NC was reduced.

#### 3.1.3. In vitro dissolution studies

Fig.3. depicts that 97% of NC was found to be dissolved

at 180 min on the other hand, only 56% of CUR was dissolved in the same period. It was observed that NC

reached 50% dissolution in 60 min; whereas CUR did not reach even 50% dissolution at 180 min.



a) curcumin showed sharp melting endothermic peak at 171.3°C, and a melting enthalpy of fusion 160.7 J/g b) nanonized curcumin showed melting endothermic peak at 176.89°C, and a melting enthalpy of fusion 65.1 J/g indicating reduced crystallinity

Fig. 2: DSC thermograms

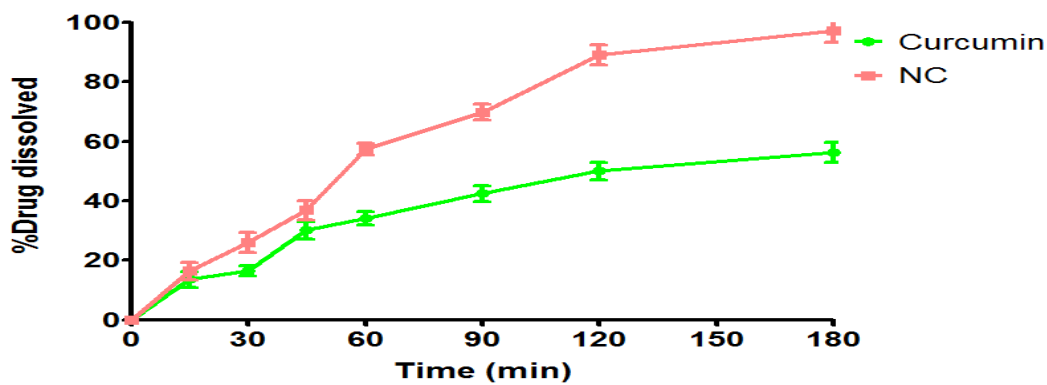


Fig. 3: Dissolution profile of curcumin and nanonized curcumin, indicating that enhanced solubility of nanonized curcumin

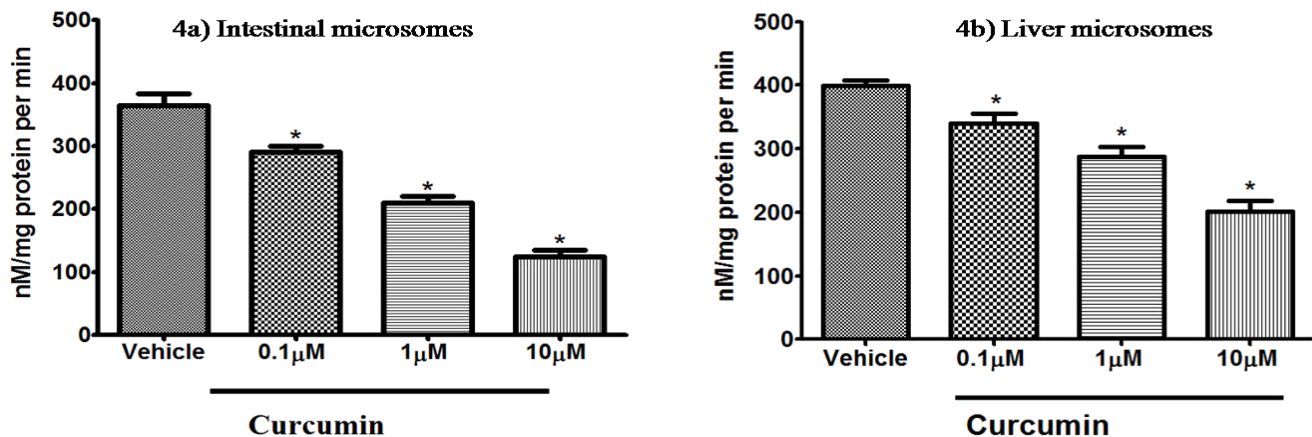
### 3.2. Assessment of *in vitro* CYP3A activity

Fig.4a and 4b exhibits the extent of erythromycin-N-demethylation (EMD) due to CYP3A activity in intestine and liver. One-way ANOVA indicates that CUR treatment significantly influenced the activity in both intestine ( $p < 0.05$ ) and liver microsomes ( $p < 0.05$ ). The post hoc test further reveals that the levels of EMD in CUR treated group at all concentrations (0.1, 1, and 10 mM) were significantly reduced ( $p < 0.05$ ) in the intestinal microsomes when compared with vehicle control. Similarly, CUR treatment significantly decreased ( $p < 0.05$ ) EMD in liver microsomes at all concentrations (0.1, 1, and 10 mM) when compared with the vehicle control.

### 3.3. Assessment of *in vivo* CYP 3A activity

The plasma concentration-time profile of midazolam in

non-dexamethasone treated control group, and dexamethasone along with CUR (60 mg/kg), NC (60 mg/kg), ketoconazole (5 mg/kg) and vehicle (0.5% methylcellulose) treated group are depicted in fig.5. The pharmacokinetic parameters of midazolam in all groups is summarised in table 1. Dexamethasone pretreatment significantly decreased  $C_{max}$  ( $p < 0.05$ ),  $AUC_{0-t}$  ( $p < 0.05$ ), of midazolam as compared to non-dexamethasone treated control group. Administration of CUR (60 mg/kg) and NC (60 mg/kg) to dexamethasone pretreated rats significantly increased the  $C_{max}$  ( $p < 0.05$ ),  $AUC_{0-t}$  ( $p < 0.05$ ) of midazolam as compared to non-dexamethasone treated control group. Similarly, administration of ketoconazole to dexamethasone pre-treated rats significantly ( $p < 0.05$ ) increased all pharmacokinetic parameters of midazolam.



Data are represented as mean  $\pm$  SD ( $n=6$ ). \* $p < 0.05$  vs. vehicle; Statistical analysis was carried out using One-Way ANOVA followed by Bonferroni multiple comparisons test

**Fig. 4: *In vitro* CYP3A inhibitory activity of curcumin on rat intestinal (4a) and liver (4b) microsomes**

**Table 1: Effect of curcumin (CUR) and nanonized curcumin (NC) on the pharmacokinetic (PK) parameters of midazolam (MDZ)**

PK parameters	Group1 MDZ Control	Group 2 (Dexa)	Group 3 (Dexa+ Cur)	Group 4 (Dexa+NC)	Group5 (Dexa+Keto)
$C_{max}$ (ng/mL)	784.15 $\pm$ 63.89	287.67 $\pm$ 18.93 <sup>#</sup>	585.01 $\pm$ 46.55*	673.65 $\pm$ 19.53*	715.68 $\pm$ 21.82*
$T_{max}$ (h)	1.0 $\pm$ 0.0	1.0 $\pm$ 0.0	1.0 $\pm$ 0.0	1.0 $\pm$ 0.0	1.0 $\pm$ 0.0
$AUC_{0-t}$ (h ng/ml)	1853.11 $\pm$ 97.24	485.26 $\pm$ 45.89 <sup>#</sup>	1046.56 $\pm$ 91.44*	1127.74 $\pm$ 68.80*	1220.96 $\pm$ 80.17*
$AUC_{0-\infty}$ (h ng/ml)	2865.78 $\pm$ 407.78	525.86 $\pm$ 61.45 <sup>#</sup>	1461.93 $\pm$ 200.83*	1775.13 $\pm$ 203.38*	2216.79 $\pm$ 268.08*
$K_e$ (h <sup>-1</sup> )	0.31 $\pm$ 0.06	0.74 $\pm$ 0.16	0.36 $\pm$ 0.06	0.28 $\pm$ 0.04	0.22 $\pm$ 0.03
$t_{1/2}$ (h)	2.26 $\pm$ 0.53	0.96 $\pm$ 0.22	1.91 $\pm$ 0.30	2.46 $\pm$ 0.42	3.13 $\pm$ 0.40
CL/F(L/h)	3.55 $\pm$ 0.47	19.24 $\pm$ 2.30	6.96 $\pm$ 1.02*	5.69 $\pm$ 0.60*	4.58 $\pm$ 0.64*

$C_{max}$ : peak plasma concentration;  $T_{max}$ : time to reach;  $AUC_{0-t}$ : area under the plasma concentration-time curve from 0 h to t;  $AUC_{0-\infty}$ : area under the plasma concentration-time curve from 0 h to infinity;  $K_e$ : elimination rate constant;  $t_{1/2}$ : terminal half-life; Data are represented as mean  $\pm$  SD ( $n = 6$ ) <sup>#</sup> $p < 0.05$  vs. MDZ control; \* $p < 0.05$  vs. dexamethasone alone group.

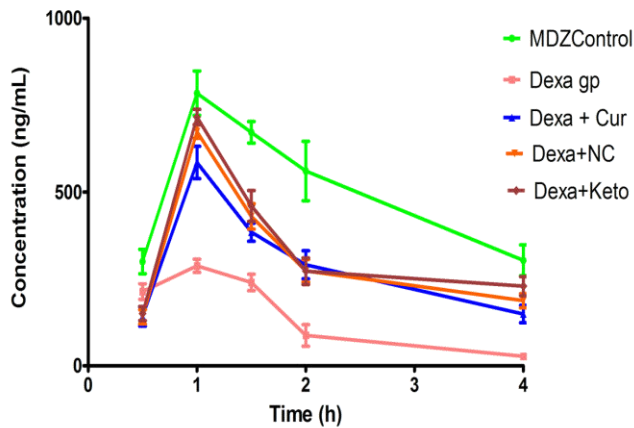
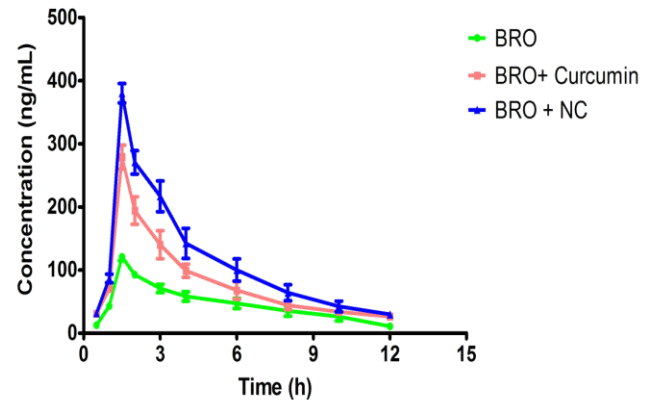


Fig. 5: Plasma concentration–time curve of midazolam (MDZ)

### 3.4. Pharmacokinetics of BRO

The mean pharmacokinetic parameters of BRO (10 mg/kg) are summarized in Table 2. Effect of CUR and NC (60 mg/kg p.o.) on the pharmacokinetics of BRO is depicted in fig. 6. Pretreatment with CUR and NC (60mg/kg, p.o) significantly ( $p < 0.05$ ) improved pharmacokinetic parameters of BRO compared with BRO alone group. The  $C_{max}$ ,  $AUC_{0-t}$  and  $AUC_{0-\infty}$  of BRO were found to be increased by 2.32, 1.72 and 1.93 fold, respectively in CUR pre-treated group compared with BRO alone group. The  $C_{max}$ ,  $AUC_{0-t}$  and  $AUC_{0-\infty}$  of BRO were found to be increased by

3.16, 2.43 and 2.48 fold, respectively in NC pre-treated group compared with BRO alone group. In CUR and NC pretreated groups, CL/F of BRO significantly decreased while there was no significant change found in  $t_{max}$  of BRO compared with BRO alone group. In addition, NC pre-treated group showed significant ( $p < 0.05$ ) improvements in the pharmacokinetic parameters of BRO compared with CUR pre-treated group.



Control group administered with BRO alone on day 11 and pre-treatment groups administered with CUR and NC for 10 days and on day11 with BRO followed by CUR and NC. Data are represented as mean  $\pm$ SD ( $n = 6$ )

Fig. 6: Plasma drug concentration-time plots of bromocriptine (BRO)

Table 2: Effect of Curcumin (CUR) and nanonized curcumin (NC) on the pharmacokinetic (PK) parameters of bromocriptine (BRO)

PK parameters	BRO	BRO+CUR	BRO+ NC
$C_{max}$ (ng/mL)	120.93 $\pm$ 5.86	279.08 $\pm$ 19.0*	380.20 $\pm$ 15.26* <sup>#</sup>
$T_{max}$ (h)	1.50 $\pm$ 00	1.50 $\pm$ 00	1.50 $\pm$ 00
$AUC_{0-t}$ (h ng/ml)	540.32 $\pm$ 63.12	933.94 $\pm$ 85.54*	1313.43 $\pm$ 147.35* <sup>#</sup>
$AUC_{0-\infty}$ (h ng/ml)	593.53 $\pm$ 50.52	1145.52 $\pm$ 98.42*	1473.78 $\pm$ 158.26* <sup>#</sup>
$Ke$ (h <sup>-1</sup> )	0.27 $\pm$ 0.11	0.19 $\pm$ 0.03	0.13 $\pm$ 0.03
$t_{1/2}$ (h)	2.87 $\pm$ 1.0	3.75 $\pm$ 0.70	5.61 $\pm$ 1.34
CL/F(L/h)	16.94 $\pm$ 1.29	8.78 $\pm$ 0.74*	6.84 $\pm$ 0.66* <sup>#</sup>

$C_{max}$ : peak plasma concentration;  $T_{max}$ : time to reach;  $AUC_{0-t}$ : area under the plasma concentration-time curve from 0 h to t;  $AUC_{0-\infty}$ : area under the plasma concentration-time curve from 0 h to infinity;  $Ke$ : elimination rate constant;  $t_{1/2}$ : terminal half-life; Data are represented as mean  $\pm$ SD ( $n = 6$ ) \* $P < 0.05$  vs control; <sup>#</sup> $P < 0.05$  vs BRO+CUR.

## 4. DISCUSSION

Curcumin exhibits wide range of therapeutic effects. However, the pharmacological use of CUR has been limited because of its low solubility in both acidic and neutral pHs. It has been reported that curcumin can be solubilized to an extent of  $< 0.6 \mu\text{g/mL}$  in pure water

and 1 mg/mL in ethanol [29]. Solubility of CUR can be improved by its nanonization.

In the present investigation, particle size of CUR was reduced to nano size and was confirmed using zetasizer in particle size analysis. Nanoparticles were found to be spherical in morphology with a narrow size distribution,



as evidenced by SEM micrographs. An amorphous or metastable form could dissolve at a faster rate because of its higher internal energy and greater molecular mobility, as compared to crystalline materials [30]. DSC analysis confirmed that NC has lower crystallinity compared to native CUR.

It is widely known that poor solubility and slow dissolution can lead to low bioavailability. Nanonization is a novel approach that improves solubility and dissolution rates of poorly soluble drugs which in turn enhances bioavailability. In our study, *in vitro* dissolution revealed that NC has higher solubility than CUR. The solubility of NC was increased because of smaller particles size as compared to CUR. An earlier study, suggests that the solubility of nano-material increases with decreasing particle size [31].

Although almost all the cytochrome P450 enzymes are present in the liver, lower concentrations of these enzymes are also present in the small intestine. Small intestine has the ability to metabolize drugs and other xenobiotics in addition to its primary role of absorption [32]. Potential inducer or inhibitor of CYP3A may decrease or increase the metabolism of CYP3A substrate drugs and consequently alter the pharmacokinetic and pharmacodynamic profiles [33]. CUR has the potential to cause herb-drug interaction when administered with other drugs.

EMD assay is an indicator of CYP3A activity. We investigated CYP3A inhibitory activity of CUR using EMD assay in which CUR has showed dose dependant inhibitory action on CYP3A enzymes. The results indicate that the intestinal CYP3A activity was inhibited to a greater extent than the liver microsomal activity, which may be attributed to the fact that intestinal microsomal preparations have a low overall concentration of CYPs in comparison to hepatic preparations [22].

The dexamethasone pretreated rat model is widely employed for evaluation of *in vivo* CYP3A inhibitors [34]. In this method, midazolam, dexamethasone and ketoconazole are used as CYP3A substrate, CYP3A inducer and CYP3A inhibitor, respectively. The plasma concentration of midazolam depends upon CYP3A activity. Dexamethasone increases the systemic concentration of midazolam by increasing its metabolism. Increased plasma concentration ( $AUC_{0-t}$ ) of midazolam in dexamethasone pretreated animals indicates that dexamethasone enhances the CYP3A enzyme activity. Animals treated with ketoconazole showed an increased plasma concentration of midazolam. In animals pre-treated with CUR and NC,

NC group showed significantly ( $p < 0.05$ ) increased plasma concentration of midazolam compared with CUR group which indicates an improved inhibitory action of NC on CYP3A enzymes. These findings further confirm and substantiate the inhibitory action of NC on CYP3A activity.

Additionally, in order to support the *in vitro* CYP3A inhibition in the rat liver and intestine and midazolam assay, we also performed *in vivo* studies in rats to evaluate the effect of CUR and NC on the pharmacokinetics of BRO. Animals pretreated with CUR and NC for a period of 10 days showed significantly increased  $C_{max}$  and AUC of orally administered BRO compared with animals treated with BRO alone group suggesting that pretreatment of CUR and NC significantly altered pharmacokinetics of BRO and enhanced its bioavailability. Animals pre-treated with NC showed significant improvement in  $C_{max}$  and AUC of orally administered BRO compared with animals pre-treated with CUR. In addition, pretreatment with CUR and NC resulted in a significant decrease in CL/F of BRO while there was no significant change found in  $t_{max}$  of BRO compared with BRO alone group. Decreased CL/F,  $k_{el}$  and increased  $t_{1/2}$  values indicating the inhibition of elimination of BRO upon CUR and NC pretreatment. Previous literature suggest that BRO is easily absorbed (65 to 95%) through the gastrointestinal tract but due to extensive first-pass metabolism in the liver (>90%), very less amount (3 to 7%) of oral dose reaches the systemic circulation [4, 35]. Based on the existing evidence, it is hypothesised that the bioavailability improvement of BRO might be due to predominant inhibition of liver CYP3A enzymes.

Curcumin has been proven for its neuroprotective activity in the treatment of Parkinson's disease. In the present study, NC significantly increased the plasma concentration of BRO. The present results suggest NC may provide additional benefits in the treatment of Parkinson's disease when it is administered with BRO. However, these findings need to be evaluated in human subjects for further confirmation.

## 5. CONCLUSION

Nanonization is a novel approach to enhance solubility of CUR there by its oral bioavailability. In the present experimental investigation, NC increased the bioavailability of BRO by inhibiting its metabolism, which is mediated through intestinal and liver CYP3A enzymes.

## 6. ACKNOWLEDGMENT

Ms. Kankalatha Alikatte, wishes to acknowledge the Department of Pharmacy, University College of Technology, Osmania University, Hyderabad, for providing registration (Reg. No 900917621044), to undertake the doctoral dissertation work.

### Conflict of interest

None of the authors has any conflict of interest to disclose. We confirm that we have read the Journal's position on issues involved in ethical publication and affirm that this report is consistent with those guidelines.

**Funding:** This work has not received grants from any funding agency.

## 7. REFERENCES

- Viney L, Dharmpal S, Deepti P. *J. Exp. Nanosci.*, 2016; **11(13)**:1044-1057.
- Schran HF, Tse FL, Bhuta SI. *Biopharm. Drug. Dispos.*, 1985; **6(3)**:301-311.
- Ralph AD. *Diabetes. Care.*, 2011; **34(4)**:789-794.
- Nelson MV, Berchou RC, Kareti D, LeWitt PA. *Clin. Pharmacol. Ther.*, 1990; **47**:694-697.
- Ravichandran R. *J. Biomater. Nanobiotechnol.*, 2013; **4**:291-299.
- Aftab N, Vieira A. *Phytother. Res.*, 2010; **24**:500-502.
- Jurenka JS. *Altern. Med. Rev.*, 2009; **14**:141-153.
- Sharma RA, Gescher AJ, Steward WP. *Eur. J. Cancer.*, 2005; **41**:1955-1968.
- Hatcher H, Planalp R, Cho J, Torti FM, Torti SV. *Cell. Mol. Life. Sci.*, 2008; **65**:1631-1652.
- Lavellea EC, Sharif S, Thomas NW, Holland J, Davis SS. *Adv. Drug. Delivery. Rev.*, 1995; **18**:5-22.
- Bezirtzoglou EEV. *Microb. Ecol. Health Dis.*, 2012; **23**:1-10.
- Appiah-Opong R, Commandeur JN, Van Vugt-Lussenburg B, Vermeulen NP. *Toxicology*, 2007; **235**: 83-91.
- Cho HJ, Yoon IS. *Evid. Based. Complement. Alternat. Med.*, 2015.
- Verma P, Pathak K. *Nanomed. Nanotechnol. Biol Med.*, 2012; **8**:489-496.
- Yadav D, Kumar N. *Int. J. Pharm.*, 2014; **477(1-2)**:564-577.
- Roopa G, Jayanthi C, Pankaj B, Roopa K, Hanumanthachar KJ, Divakar G. *Micro. Nanosys.*, 2017; **9(2)**:1-9.
- Saha S, Ramesh R. *Int. J. Chemtech. Res.*, 2015; **7(4)**: 616-628.
- Tripathi A, Gupta R, Saraf SA. *Int. J. Pharm.Tech. Res.*, 2010; **2(3)**:2116-2123.
- Hasan M, Elkhoury K, Kahn CJF, Arab-Tehrany E, Linder M. *Molecules*, 2019; **24(10)**:2023.
- Wrighton SA, Schuetz EG, Watkins PB, Maurel P, Barwick J Bailey BS, et al. *Mol. Pharmacol.*, 1985; **28**:312-321.
- Nash T. *Biochem. J.*, 1953; **55**:416-421.
- Cotreau MM, Von Moltke LL, Beinfeld MC, Greenblatt DJ. *J. Pharmacol. Toxicol. Methods*, 2000; **43**:41-54.
- Takemoto K, Yamazaki H, Tanaka Y, Nakajima M, Yokoi T. *Xenobiotica*, 2003; **33**:43-55.
- Wolfson WQ, Chon C. *Am. J. Clin. Pathol.*, 1948; **18(9)**:723-730.
- Schenkman JB, Cinti DL. *Methods. Enzymol.*, 1978; **52**:83-89.
- Kanazu T, Yamaguchi Y, Okamura N, Baba T, Koike M. *Xenobiotica*, 2004; **34**:403-413.
- Yamano K, Yamamoto K, Kotaki H, Takedomi S, Matsuo H, Sawada Y, et al. *J. Pharmacol. Exp. Ther.*, 2000; **292**:1118-1126.
- Choi YJ, Seo MK, Kim IC, Lee YH. *J. Chromatogr.*, 1997; **694**:415-420.
- Kurien BT, Singh A, Matsumoto H, Scofield RH. *Assay. Drug. Dev. Technol.*, 2007; **5(4)**:567-576.
- Hancock BC, Zografi G. *J. Pharm. Sci.*, 1997; **86**:1-12.
- Keck CM, Muller RH. *Eur. J. Pharm. Biopharm.*, 2006; **62**:3-16.
- Lin JH, Chiba M, Baillie TA. *Amer. Soci. Pharmacol. Exp. Ther.*, 1999; **51(2)**:135-157.
- Chaobal HN, Kharasch ED. *Clin. Pharmacol. Ther.*, 2005; **78**:529-539.
- Marathe PH, Rodrigues AD. *Curr. Drug. Metab.*, 2006; **7**:687-704.
- Shivaprasad C, Kalra S. *Indian. J. Endocrinol. Metab.*, 2011; **15(Suppl 1)**:S17-S24.